Applied Thermal Engineering 127 (2017) 1543–1554

Contents lists available at ScienceDirect

Applied Thermal Engineering

journal homepage: www.elsevier.com/locate/apthermeng

Research Paper

A small-scale solar organic Rankine cycle combined heat and power system with integrated thermal energy storage

J. Freeman [a], I. Guarracino [a], S.A. Kalogirou [b], C.N. Markides [a,*]

[a] Clean Energy Precesses (CEP) Laboratory, Department of Chemical Engineering, Imperial College London, South Kensington Campus, London SW7 2AZ, UK
[b] Department of Mechanical Engineering and Materials Science and Engineering, Cyprus University of Technology, 45 Kitiou Kyprianou Street, 3041 Limassol, Cyprus

HIGHLIGHTS

- Thermal energy storage solutions for a domestic-scale solar CHP system are compared.
- The system includes a 15-m^2 solar collector array and an ORC engine.
- Diurnal and seasonal performance in the climates of Cyprus and the UK are assessed.
- Phase change materials are compared to conventional thermal energy storage options.
- Hydrated-salt PCMs show the highest electrical work output per unit storage volume.

ARTICLE INFO

Article history:
Received 6 March 2017
Revised 24 May 2017
Accepted 21 July 2017
Available online 22 July 2017

Keywords:
Renewable technologies
Solar power
Solar thermal
Domestic
Combined heat and power
Organic Rankine cycle

ABSTRACT

In this paper, we examine integrated thermal energy storage (TES) solutions for a domestic-scale solar combined heat and power (S-CHP) system based on an organic Rankine cycle (ORC) engine and low-cost non-concentrating solar-thermal collectors. TES is a critical element and distinct advantage of solar-thermal systems. It can allow, depending on how it is implemented, improved matching to the end-user demands, improved load factors, higher average efficiencies and overall performance, as well as reduced component and system sizes and costs, especially in climates with high solar-irradiance variability. The operating temperature range of the TES solution must be compatible with the solar-collector array and with the ORC engine operation in order to maximise the overall performance of the system. Various combinations of phase change materials (PCMs) and solar collectors are compared and the S-CHP system's performance is simulated for selected months in the contrasting climates of Cyprus and the UK. The most important performance indicator of the ORC engine, i.e., net-power output, and the required TES volume are compared and discussed. The PCM-TES solutions that enable the best summer performance from an ORC engine sized for a nominal ~1-kW_e output in combination with a 15-m^2 solar collector array result in diurnal volume requirements as low as ~100 L in Cyprus and 400–500 L in the UK. However, the required TES volume is strongly influenced by the choice of operational strategy for the system in matching the domestic load profiles. In a full-storage strategy in which electrical energy generation from the ORC engine is offset to match the week-day evening peak in demand, it is found that a ~20% higher total daily electrical output per unit storage volume can be achieved with a PCM compared to water as a sensible storage medium. The isothermal operation of the PCMs during phase-change allows for smaller diurnal storage temperature swings and higher energy conversion efficiencies from the solar collector array. These results are useful in informing the development of small-scale solar-thermal heat and power systems and of suitable integrated TES solutions for such applications.
© 2017 The Authors. Published by Elsevier Ltd. This is an open access article under the CC BY license (http://creativecommons.org/licenses/by/4.0/).

1. Introduction

Solar-thermal power systems have the potential to provide clean energy in the form of electricity, along with useful heat (for domestic hot water and/or space heating), across a wide range of scales and applications [1,2]. Steam-Rankine and, to a lesser extent, Stirling-engine systems are proven technologies for use with medium- and high-temperature concentrating solar-thermal collectors, as are organic Rankine cycle (ORC) systems, which show strong potential for use in small-scale systems (<10 kW_e) with lower-temperature, non- or low-concentrating collectors [3,4].

* Corresponding author.
E-mail address: c.markides@imperial.ac.uk (C.N. Markides).

http://dx.doi.org/10.1016/j.applthermaleng.2017.07.163
1359-4311/© 2017 The Authors. Published by Elsevier Ltd.
This is an open access article under the CC BY license (http://creativecommons.org/licenses/by/4.0/).

Nomenclature

Symbols

A	area, m^2
c	specific heat capacity, J kg^{-1} K^{-1}
c_1	collector heat-loss coefficient, W m^{-2} K^{-1}
c_2	temperature dependence of the heat-loss coefficient, W m^{-2} K^{-2}
h	specific enthalpy, J kg^{-1}
G	solar irradiance, W m^{-2}
K_θ	collector incident angle modifier (IAM), –
$\dot{m}$	mass flow-rate, kg s^{-1}
T	temperature, K
t	time, s
Q_u	collector thermal energy (heat) output, J
U	internal energy, J
W	work, J
$\dot{W}$	power, W
β	collector inclination angle, °
ρ	density, –
η_0	solar collector optical (zero-loss) efficiency, –
η_{ov}	overall solar-to-electrical efficiency, –
θ	solar incidence angle, °

Subscripts

a	ambient air
b	beam
app	approach
avg	average
avg-day	average day
cond	condensation
d	diffuse
e	electrical
exp	expander
evap	evaporation
fs	full storage
in, out	inlet, outlet
net	net power
ORC	organic Rankine cycle
PCM	phase change material
pc	phase change
pp	pump
ps	partial storage
r	refrigerant working fluid
sc	solar collector
sup	superheat
TES	thermal energy store
1, 2, 3, 4	cycle state points

In earlier work [5,6], the authors presented a thermoeconomic investigation of a domestic-scale solar combined heat and power (S-CHP) system based on an ORC engine, taking a thermal input from a 15-m^2 rooftop array of non-concentrating solar-thermal collectors. The potential of this technology as a viable alternative to solar-PV systems was found to be highly dependent on: (i) its potential to achieve a low cost of electricity through the use of low-cost components, in particular the solar collectors and the ORC expander; (ii) its ability to generate variable quantities of heat or power to suit the varying household demands; and (iii) its distinct and highly advantageous ability to use low-cost thermal energy storage (TES) to provide continuous operation under intermittent solar-irradiance conditions and to offset the periods of electrical and thermal energy provision to the time of day at which they are most valuable.

A wide-range of TES solutions are being considered for use with solar-thermal power systems. Conventional TES solutions for large-scale concentrating solar power (CSP) systems featuring steam-Rankine power plants typically use indirect two-tank systems, providing storage for periods of 6–12 h operation at full capacity. In this arrangement, a molten-salt mixture is pumped, during the charging cycle, from a cold-storage tank to a hot-storage tank via a heat exchanger where it is heated by a heat-transfer oil from the solar field. In order to deliver superheated steam at 100 bar, the temperatures of the salts in the hot- and cold-storage tanks need to be in the region of 390 °C and 300 °C, respectively [7]. Single-tank thermocline systems are sometimes considered as a lower-cost alternative to two-tank systems, and low-cost filler materials such as quartzite and granite particles are often included to provide a higher specific heat capacity and to reduce the required storage volume and cost of additional heat-transfer fluid [8,9].

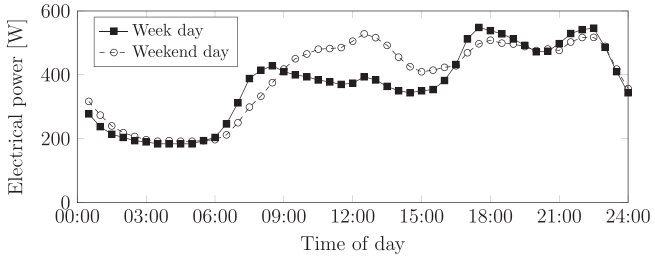
ORC systems tend to be smaller than steam-Rankine cycle power plants, and are typically designed for operation at lower temperatures with suitably-selected working fluids. Chacartegui et al. [10] investigated two TES configurations for use in a 5-MW_e CSP-ORC system with a design solar-array outlet temperature of 400 °C. These were an indirect two-tank configuration, similar to that described above, and a direct two-tank configuration in which the TES media (a eutectic mixture of sodium-nitrate and potassium-nitrate salts) was also used as the heat-transfer fluid to be circulated through the solar field. The direct-storage configuration was found to require a smaller tank volume and a lower investment cost, while the addition of TES was found to reduce the system's cost of electricity. The earliest example of a modern solar-ORC power plant is the demonstration plant in Saguaro, Arizona, featuring a 10,000-m^2 PTC field with a design outlet temperature of 300 °C and an ORC system with a turbine expander and pentane as the working fluid [11]. The plant was originally installed without TES, however, a thermocline TES with gravel as the filler material has been proposed for a future retrofit [12]. A similar single-tank packed bed TES concept was also proposed by Quoilin et al. [13] for a smaller (3 kW) rural solar-ORC system in Lesotho, Africa, while Casati et al. [14] proposed a range of direct-storage concepts for ORC systems in which the ORC working fluid is stored in two-phase equilibrium in a TES tank, for extraction either in the liquid or vapour phase, before being fed to the expander (after an intermediate flashing process in the liquid case). Disadvantages with this approach are the lower energy density and the challenge of maintaining a constant pressure in the TES vessel.

A number of investigators have proposed TES solutions for solar systems using solid-liquid phase change materials (PCMs). Such materials are chosen to absorb a significant amount of heat as they undergo the melting process (from solid to liquid), over a narrower temperature range than would be achieved by sensible TES in an equivalent volume. PCMs are broadly divided into a wide range of organic compounds (such as waxes, fatty acids and glycol-based compounds) and inorganic salt-hydrates. PCM-TES solutions studied in the literature often feature embedded heat exchangers [15,16], or the PCM encapsulated in small containers, immersed within larger tanks to enhance the thermal storage capacity and

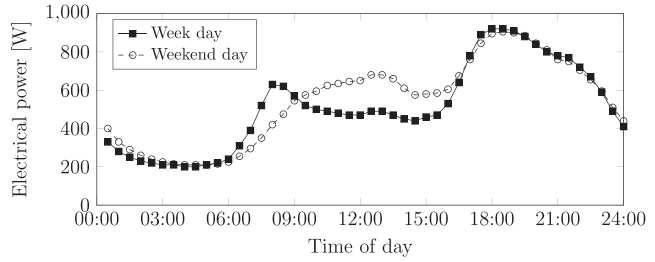
heat transfer over a given temperature range [17]. Naghavi et al. [18] proposed the incorporation of PCMs into the manifold of an evacuated-tube heat-pipe solar collector and compared its simulated performance to a typical collector with a hot-water storage tank arrangement. The PCM system used paraffin wax with a melting temperature of 64 °C, and was found to offer a larger useful daily energy output compared to the conventional hot-water system that was found to suffer significant thermodynamic losses due to destratification over the diurnal storage period. Steinman and Eck [19] proposed the use of encapsulated PCM in steam accumulators, in order to provide process steam at constant temperature and pressure. A similar concept was also considered for a solar ORC system by Jing et al. [20], in order to provide a constant vapour quality to the expander under varying solar conditions.

When considering energy storage for a domestic distributed-power application, detailed consideration must be given to the electricity load profile. The typical annual electricity consumption for a UK home, according to OFGEM, is 3100 kW h yr^{-1} (or, 354 W, average) [23]. For homes with multi-rate meters where electrical storage heaters tend to be used for heating, the typical annual consumption is 4300 kW h yr^{-1} (491 W, average), however, this accounts for less than 10% of homes in the UK [24]. Diurnal domestic electricity-load profiles for the UK typically show a characteristic peak in consumption in the early evening occurring between 16:30 and 19:30 [24,25], although the exact shape of the load profile is dependent both on the time of the year, and the day of the week, as shown in Fig. 1. Week-day load profiles tend to show a second smaller peak in consumption occurring at around 08:00. At weekends, a daytime peak is also seen between 12:00 and 13:00.

At more southerly geographical locations that experience higher levels of solar irradiation and higher ambient temperatures, the domestic electricity demand is affected by the requirement for air conditioning. Serghides et al. [26] found from a study of 104 dwellings in Cyprus that homes with air-conditioning (85% of those surveyed) had more than double the annual electricity consumption of those without, on average. The use of air conditioning also affects the characteristic shape of the domestic load profile. Fig. 2 shows that the shape of the week- and weekend-day electricity load profiles for Cyprus in the winter are similar to those for the UK, with the major peak occurring at around 18:30. In the summer, the profile is generally flatter than for the UK with a higher overnight consumption (corresponding to air conditioning) and a mid-afternoon peak between the hours of 15:00 and 17:00 that is not encountered in the UK.

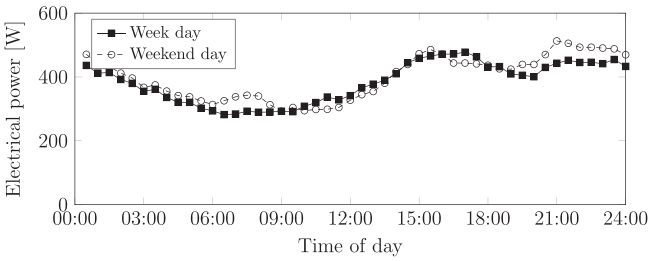


(a) Summer domestic load profile, UK.

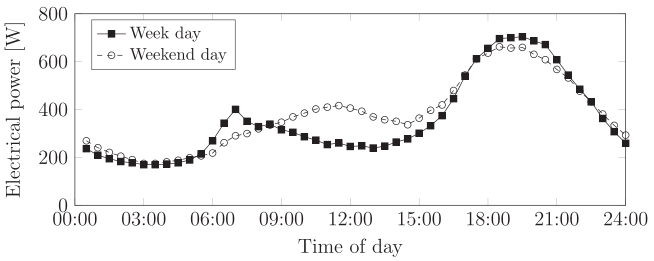


(b) Winter domestic load profile, UK.

Fig. 1. UK average week- and weekend-day household electricity consumption profiles in: (a) summer (mid May to early September) and (b) winter (late October to late March) [21].



(a) Summer domestic load profile, Cyprus.



(b) Winter domestic load profile, Cyprus.

Fig. 2. Cyprus average week- and weekend-day household electricity consumption profiles in: (a) summer and (b) winter [22].

In this work we aim to assess a range of TES media for use in a domestic S-CHP system based on a solar-collector array and an ORC engine, with particular attention given to PCMs as storage media. Of particular importance is the determination of appropriate storage temperatures that maximise the overall solar-to-electrical conversion efficiency of the S-CHP system, which is considered in two contrasting seasonal climates of Cyprus and the UK. The required TES volumes and system operational strategies are also considered in order to provide the best match between the systems' electrical outputs and the domestic seasonal load-profiles in the respective locations.

2. Methodology

Fig. 3 shows the layout of the S-CHP system of interest. A TES vessel acts as the interface between the ORC engine and the

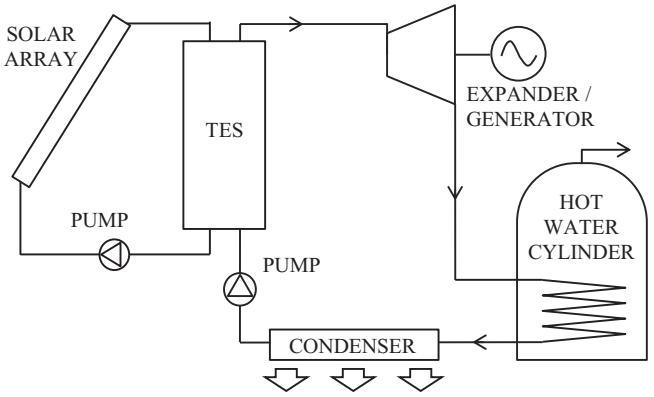


Fig. 3. Schematic of the S-CHP system with TES vessel.

solar-collector array, while serving as the evaporator heat-exchanger for the ORC engine. A calorifier is also included for the provision of domestic hot-water (DHW) from the heat rejected by the ORC condenser, although the present analysis focuses on the system's electrical output. The overall aim of this paper is to consider the TES material, associated storage volume and operating temperatures that result in the maximum net-work output from the S-CHP system. To perform this analysis, sub-system models of the solar-collector array, ORC engine and TES vessel are developed, and these are presented below.

2.1. Solar collector sub-system

The present study considers two types of non-concentrating collector: (i) a new-generation, high-performance evacuated flat-plate collector (EFPC) developed especially for medium temperature process-heating applications (including ORC systems) [27]; and (ii) a standard, lower-cost evacuated-tube heat-pipe collector (ETHPC) designed for low-temperature DHW heating applications [28]. The collector array is modelled as south-facing, with an inclination angle of 36° for the UK and 30° for Cyprus (chosen to maximise the total annual irradiation for each location). The total array size is constrained to within the dimensions of a typical domestic roof-space, taken as 15 m^2 [29]. The solar-collector array is modelled as operating under quasi-steady state conditions, with the thermal capacity of the collectors neglected. It is assumed in the sizing calculations that the collector sub-system is operational only for the hours of the day when the solar incidence angle on the tilted collector plane is <70°.

The performance of the solar-collector array is estimated using hourly climate data for London, UK and Larnaca, Cyprus [30]. The collectors are modelled using a steady-state efficiency equation:

$$\frac{\dot{Q}_u}{A_{sc}} = \eta_0\left(K_{\theta,b}G_b + K_{\theta,d}G_d\right) - c_1\left(\overline{T}_{sc} - T_a\right) - c_2\left(\overline{T}_{sc} - T_a\right)^2, \quad (1)$$

where η_0 is the zero-loss optical efficiency, c_1 and c_2 are heat loss coefficients and $K_{\theta,b}$ and $K_{\theta,d}$ are incident angle modifier (IAM) factors applied to the zero-loss efficiency for the beam and diffuse components of the solar irradiance, respectively. Each of the parameters in Eq. (1) are determined experimentally as part of the Solar Keymark certification scheme, for which the testing procedures are described in European Standard EN 12975-2 [31,32]. Eq. (1) is solved by assuming that the inlet fluid-temperature is equal to the temperature of the lumped/uniform TES tank (see Section 2.3):

$$T_{sc,in} = T_{TES}. \quad (2)$$

Thus, the useful solar-energy gain is a function of both the choice of the collector (Table 1) and of the TES medium that governs the operating temperature of the solar-collector array.

2.2. Organic Rankine cycle sub-system

The cycle model and parameters used for the thermodynamic analysis of the ORC system are illustrated in Fig. 4. For full details on the ORC system modelling, the reader is referred to previous work by the authors [5,6]. In the present work, the hydrofluorocarbon R245fa is taken as the ORC working-fluid, which has been previously investigated for use in low-temperature solar-ORC systems [13,33] and has a critical temperature of 154 °C.

Table 1
Solar collector efficiency curve parameters (gross area basis). These values have been derived from the information in Refs. [27,28].

	EFPC	ETHPC
Model	TVP Solar HT-Power	Thermomax HP-200
η_0	0.774	0.556
c_1	0.376 W m^{-2} K^{-1}	0.888 W m^{-2} K^{-1}
c_2	0.006 W m^{-2} K^{-2}	0.006 W m^{-2} K^{-2}

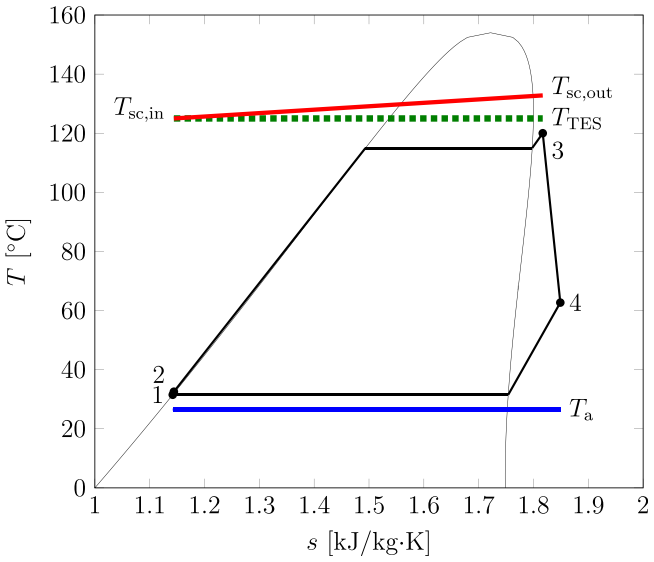


Fig. 4. *T-s* diagram of solar-TES-ORC processes, for R245fa as the ORC working fluid and a PCM as the TES medium. The following input parameters are used for the ORC analysis: η_{pp} = 65%, η_{exp} = 75%, ΔT_{app} = 5 K and ΔT_{sup} = 5 K.

The evaporator and condenser heat-exchangers are both modelled using approach temperature differences of 5 K at the working-fluid outlet, with the heat-source temperature equal to that of the TES tank:

$$T_3 = T_{TES} - 5\ \text{K}, \quad (3)$$

and cold-sink temperature equal to the maximum ambient air temperature:

$$T_1 = T_{a,max} + 5\ \text{K}. \quad (4)$$

A minimum of 5 K of superheating is also chosen for the evaporator, while for the condenser it is assumed that working fluid exits in a saturated liquid state (zero subcooling). Isentropic efficiencies of 65% and 75% are chosen for the ORC pump and expander, respectively.

The key parameters of interest for the sizing of the ORC engine in conjunction with the TES tank are the working-fluid mass flow-rate and the evaporation temperature. The evaporation temperature is set to be 10 K below the minimum operating TES temperature, while the mass flow-rate is a function of the TES storage capacity and the required period of discharge. The net-work output from the ORC engine is calculated as the expander work-output minus the pump work-input:

$$\dot{W}_{net} = \dot{m}_r[(h_3 - h_4) - (h_2 - h_1)]. \quad (5)$$

2.3. Thermal energy storage sub-system

All calculations performed in this paper use a lumped model for the TES vessel, assuming uniform temperature, with thermal losses to the environment neglected. Where PCMs are considered as the storage media, the thermal store is set to begin each day in a fully discharged (solidified) state, and the total latent heat capacity of the TES is given by:

$$Q_{pc} = V\rho\Delta h_{pc}. \quad (6)$$

where Δh_{pc} is the latent heat of fusion of the PCM in kg m^{-3}. In Section 3.5, PCMs will be compared to various sensible storage

media by way of a diurnal simulation. For this analysis the sensible storage capacity of the PCM in the liquid phase will also be considered:

$$Q_{\text{sens}} = V\rho c_{\text{p}}(T_{\max} - T_{\min}). \tag{7}$$

where $T_{\min}$ and $T_{\max}$ are the maximum and minimum temperatures of the TES over the duration of the charge/discharge cycle.

2.4. System sizing calculations

In Section 3.3, two strategies will be investigated for the sizing of the S-CHP system and the TES vessel, with PCMs as the storage media. The first is based on a "partial-storage" strategy, in which TES is used to buffer variations in solar irradiance such that the ORC engine operates for a sustained period at its design-point condition, avoiding intermittency and part-load conditions due to variations in the thermal input. For this strategy it will be assumed that the ORC engine is operational during the core daylight hours, which will be defined as the hours when the solar incidence angle on the tilted collector plane is <70° (approximately 08:00 to 17:00 in summer). The ORC engine is therefore sized for the mean solar-thermal input during the core daylight hours, $\dot{Q}_{\text{u,avg}}$, while the required volume of PCM is calculated as the difference between in solar-energy gain on the average and the peak solar day for each seasonal period:

$$\dot{m}_{\text{r,ps}} = \frac{\dot{Q}_{\text{u,avg}}}{h_3 - h_2}, \tag{8}$$

$$V_{\text{TES,ps}} = \frac{Q_{\text{u,(peak-day)}} - Q_{\text{u,(avg-day)}}}{(\rho \cdot \Delta h_{\text{pc}})_{\text{PCM}}}. \tag{9}$$

The second strategy is a "full-storage" solution in which the TES is used to shift the operating period of the ORC engine away from the core daylight hours to coincide with the evening peak in electricity demand. This strategy results in shorter operational periods for the ORC engine, which can therefore be sized for higher instantaneous power outputs. By default, the evening peak electricity demand is assumed to occur over a three-hour period in the evening, and the PCM volume is calculated so as to store the full quantity of solar energy received during daylight hours on an average solar day:

$$\dot{m}_{\text{r,fs}} = \frac{Q_{\text{u,(avg-day)}}}{(h_3 - h_2) \cdot \Delta t_{\text{peak}}}, \tag{10}$$

$$V_{\text{TES,fs}} = \frac{Q_{\text{u,(avg-day)}}}{(\rho \cdot \Delta h_{\text{pc}})_{\text{PCM}}}, \tag{11}$$

where $\Delta t_{\text{peak}} = 3$ h is the duration of the peak electricity-demand period.

The overall solar-to-electrical conversion efficiency of the system is finally evaluated as the net-work output from the ORC engine divided by the total irradiation received by the collector array:

$$\eta_{\text{ov}} = \frac{\sum \dot{m}_{\text{r}}(h_3 - h_4)}{\sum GA_{\text{sc}}}. \tag{12}$$

3. Results and discussion

3.1. Climate characteristics

In order to understand the difference in solar energy storage requirements for Cyprus and the UK, the irradiance characteristics of the two climates are compared. Fig. 5 shows the solar irradiation

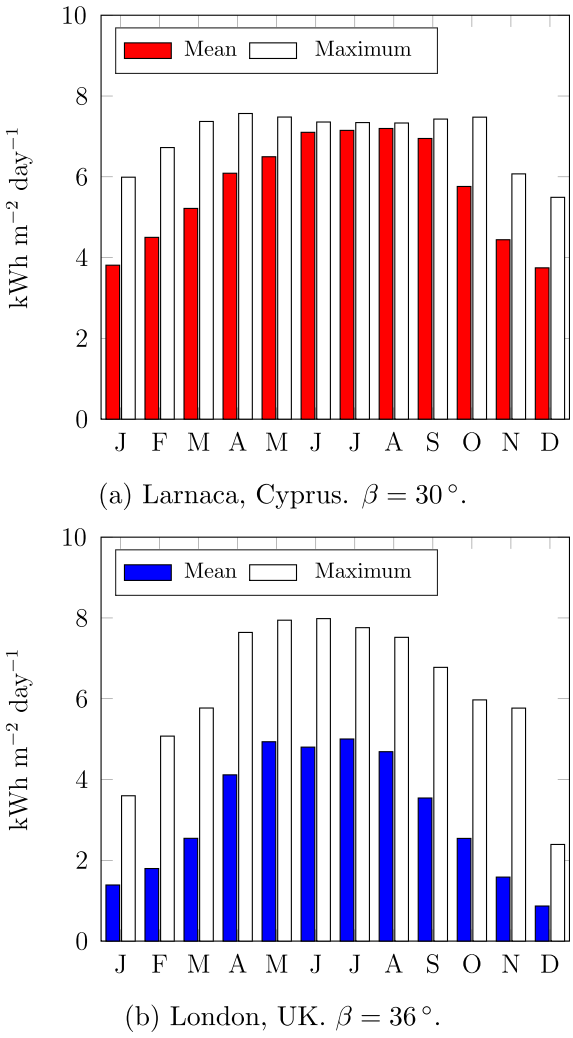


Fig. 5. Mean and maximum daily global solar irradiation values for each month of the year in: (a) Larnaca and (b) London. Irradiation values are computed for a south-orientated plane inclined at an angle β chosen to maximise the total annual irradiation for each location.

on the average day and peak day for each month of the year in Larnaca and London, respectively. The plots confirm that the Cyprus solar resource is both more abundant and undergoes less variation on a daily and seasonal timescale than the UK. In Larnaca the mean daily irradiation on the tilted plane is 5.7 kW h m^{-2} day^{-1} compared to 3.2 kW h m^{-2} day^{-1} for London. The variation in daily irradiation for Larnaca is far smaller in summer than in winter, with a standard deviation of 0.2 kW h m^{-2} day^{-1} (3%) between the months of June to August; compared to 1.9 kW h m^{-2} day^{-1} (39%) over the same period for London. Thus a TES system designed to buffer daily variations in solar gain in Cyprus can be significantly smaller than one designed for the UK, and furthermore, can be significantly reduced in size if it is designed for summer-only operation compared to year-round operation, which is not true for the UK.

3.2. Optimal storage temperature for S-CHP system operation

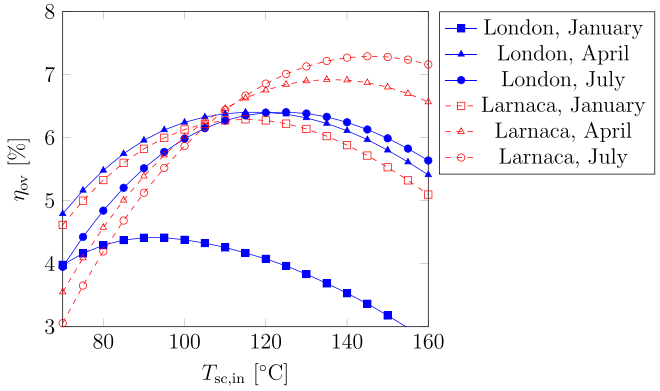
For the S-CHP system, the solar collection efficiency is highly dependent on the temperature of the heat transfer fluid exiting the TES and entering the solar-collector array. Thus a higher storage temperature results in a higher fluid temperature entering the collector array and a lower solar-energy gain. However, a

higher TES temperature also allows the ORC engine to operate with a higher evaporation temperature resulting in a higher thermal efficiency for the cycle. For example, with R245fa as the working fluid, the ORC thermal efficiency increases from 10.9% at $T_{evap} = 100\,^{\circ}C$ to 13.2% at $T_{evap} = 130\,^{\circ}C$.

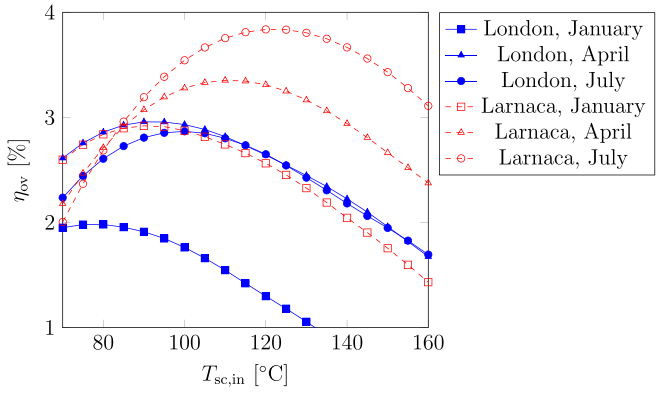
Fig. 6 shows the variation in the overall monthly solar-to-electrical conversion efficiency (ratio of total work generated to the total solar irradiation for the specified month) as a function of the chosen collector inlet-temperature for the months of January, April and July. For the S-CHP system configured with an EFPC solar-array (Fig. 6a), the optimal inlet temperature calculated for the UK ranges from 95 °C in January to 125 °C in July, resulting in maximum overall conversion efficiencies of 4.4% and 6.4% respectively. For Cyprus, higher optimal inlet temperatures of 115 °C in January and 145 °C in July result in maximum overall conversion efficiencies of 6.3–7.3%.

The ETHPC-based system is shown to deliver considerably lower efficiencies (approximately half) than the EFPC system throughout the year in both the UK and Cyprus climates. Fig. 6b shows that the maximum overall efficiency of the S-CHP system with the ETHPC solar-array is obtained at fluid inlet-temperatures 15–25 K lower than with the EFPC array. The difference in the collector efficiency between the EFPC and ETHPC is more significant at higher collector inlet-temperatures.

In Fig. 7, the useful solar-energy gain corresponding to maximum overall efficiency (at the corresponding optimum collector/storage temperature) are shown for each month for the two collector types. The useful solar-energy gain on the monthly average day (solid bars) is compared to that for the monthly peak day (dashed bars). The difference in solar-energy gain between the UK and Cyprus is more significant for winter than summer. Considering a system designed for summer operation: a TES vessel sized for full storage on the average day in July would be 60–80% larger for Cyprus than for the UK due to its higher average daily irradiation. However, the difference between the solar energy collected on the average and peak days in July is only 5–7% in Cyprus, and therefore a vessel sized according to the partial storage strategy in summer (see Eq. (8)) can potentially be an order of magnitude smaller than one sized for full storage. By comparison for the UK, there is a far larger difference in solar-energy gain between the average and peak days in the summer months, resulting in similar storage volumes required for both the full storage and partial storage strategies.

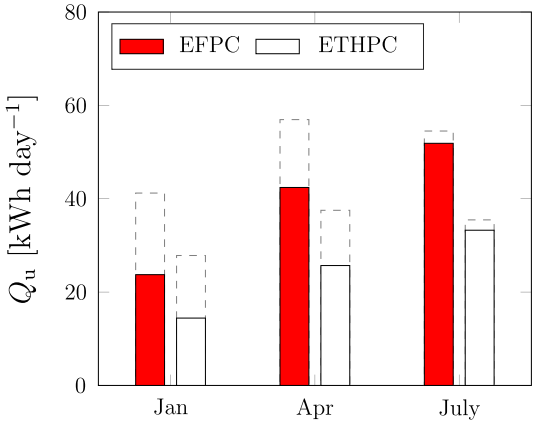


(a) Evacuated flat-plate collector (EFPC).

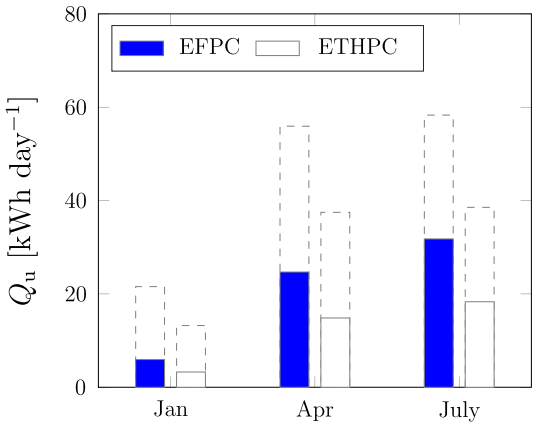


(b) Evacuated-tube heat-pipe collector (ETHPC).

Fig. 6. Overall solar-to-electrical efficiency as a function of solar collector inlet-temperature for the months of January, April and July. System simulations are performed at hourly time-intervals using full time-varying climate data for each month. Curves are plotted for the two types of solar collector: (a) EFPC and (b) ETHPC, and for operation in the climates of London, UK and Larnaca, Cyprus.



(a) Larnaca, Cyprus.

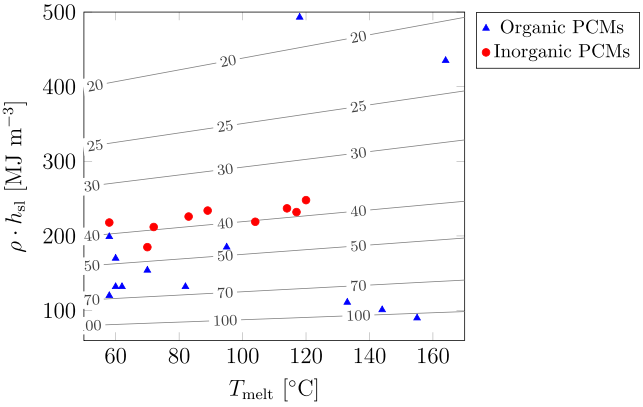


(b) London, UK.

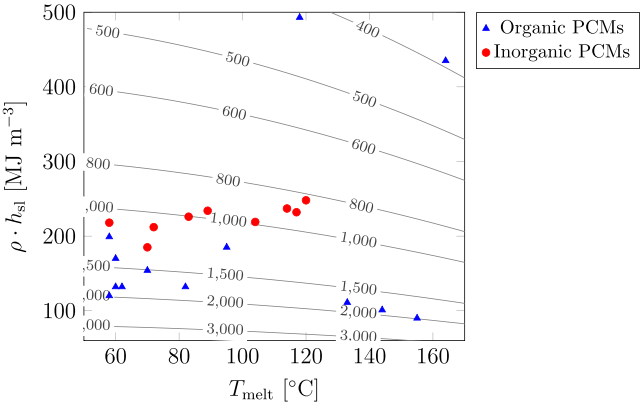
Fig. 7. Useful solar-energy gain as a function of collector type, TES medium and month of the year for: (a) Larnaca and (b) London. Bars with solid outline show the solar energy calculated for an average day in each month with the collector operating at the optimum inlet temperature (determined from Fig. 6). Bars with dashed outline show the solar energy collected on the peak solar day.

3.3. PCM storage volume requirement

In this section we focus on PCMs as the thermal storage media. Figs. 8 and 9 show the required PCM storage volume calculated for summertime in the Cyprus and UK climates respectively, as a function of the PCM melting temperature and volumetric heat capacity.

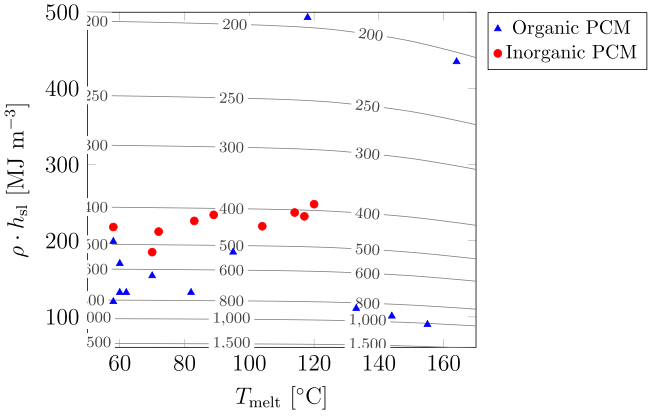


(a) Partial storage, Cyprus.

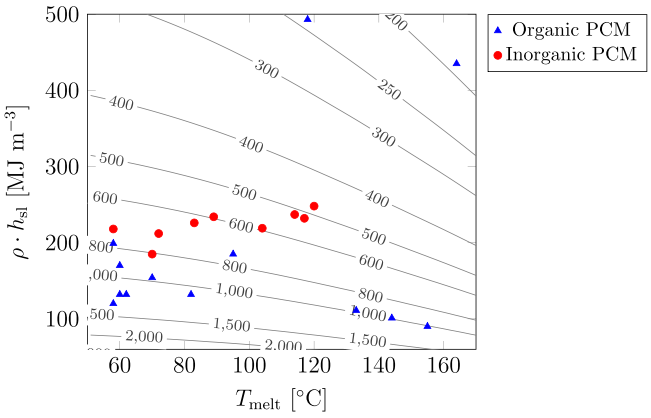


(b) Full storage, Cyprus.

Fig. 8. Required storage volume for Larnaca, Cyprus, summertime (July), as a function of PCM melting temperature (*x*-axis) and volumetric latent-heat (*y*-axis), with contour lines denoting the required storage volume (in L). The TES is sized according to: (a) the partial-storage strategy and (b) the full-storage strategy. Individual points show existing organic and inorganic PCM products.



(a) Partial storage, London.



(b) Full storage, London.

Fig. 9. Required storage volume for London, UK, summertime (July), as a function of PCM melting temperature (*x*-axis) and volumetric latent-heat (*y*-axis), with contour lines denoting the required storage volume (in L). The TES is sized according to: (a) the partial-storage strategy and (b) the full-storage strategy. Individual points show existing organic and inorganic PCM products.

For both climates, the required storage volumes for the partial-storage and full-storage strategies are compared. For the full-storage strategy, higher PCM melting temperatures lead to smaller storage volume requirements because the lower solar collector efficiency means that the daily solar energy yield is also lower. For the partial-storage strategy the melting temperature has a smaller effect on storage volume because the TES is sized for the difference in the solar energy yield between the peak and average days rather than the total. The required storage volume is also highly dependent on the volumetric latent heat of the PCM, shown on the *y*-axis. A range of existing organic and inorganic PCM products with known heat capacities and melting temperatures are also shown in the plots. It can be observed that inorganic PCMs typically have higher volumetric heat capacities during phase change (200–250 MJ m^{-3}) than the majority of the organic PCMs (100–200 MJ m^{-3}). Two of the organic PCMs are shown to have volumetric heat capacities far higher than the other organic and inorganic PCMs (>400 MJ m^{-3}). Consultation with the suppliers revealed that these PCMs are sugar-derivative products which are generally not recommended for use in applications with variable heat source (such as solar-thermal) due to their limited safe operation at temperatures above the phase change temperature [34].

The optimal PCM melting-temperature that corresponds to the maximum overall efficiency from the EFPC system designed for Cyprus in July is 145 °C, as shown in Fig. 6a. Fig. 8 shows that existing PCM products with melting temperatures close to this optimal value are organic PCMs with volumetric latent-heat around ~100 MJ m^{-3}. This results in PCM storage volumes of around ~100 L for partial storage, or 1500–2000 L for full storage. Similarly for London, the optimal PCM melting temperature for operation in July is 125 °C, again as shown in Fig. 6a. Fig. 9 indicates that the closest existing (inorganic) PCM products result in a TES volume of ~400 L for partial storage, or ~500 L for full storage. It is important to recognise here that large storage volumes are not always easily accommodated in domestic-scale applications, with hot water storage tanks for single-family residences typically holding 100–300 L. Larger storage tanks for hot and cold water supplies are often located on rooftops in Cyprus, however, this is less common in the UK [35,36].

3.4. Operational strategy and ORC sizing

At present, positive-displacement expanders as "off-the-shelf" commercially-available components for ORC systems are available at capacities of 1 kW and above [37,38]. In the following analysis, 1 kW will be considered as the lower limit for the nominal power-output from the ORC expander in S-CHP system. For the UK, the useful energy collected by the EFPC array over the average day in July is sufficient to provide almost 4 h of continuous operation from the ORC when sized for a 1-kW nominal output, which can be offset to the early evening to cover the week-day peak in

demand (see Fig. 1a). For the average day in April, sufficient energy is collected to provide a shorter duration of 3 h power provision. However, the energy yield in January is considerably lower and only sufficient to provide 45 min of continuous operation. Thus, the full-storage strategy with an appropriately-sized ORC engine shows potential for the UK as a means of offsetting solar-power provision to match the domestic peak in demand in summertime (although it is noted that in wintertime, when the evening peak demand is larger, the potential for load-profile matching is considerably lower).

In the Cyprus climate, the S-CHP system with the EFPC array and an ORC sized for a 1-kW nominal expander-power has the potential to provide 7 h of continuous power output for the average day in July, and 5 h and 3 h in April and January, respectively. However, the storage volume required to store the entire quantity of useful energy collected during daylight hours is prohibitively large for July (1.5–2 m^3 with the organic PCM closest to the optimal melting temperature), and thus in order to make full use of this use of this energy without a larger thermal store the preferred mode of operation is to run the ORC engine during the day. Furthermore, the flatter summertime load profile for Cyprus (Fig. 2a) suggests that a partial-storage strategy may be more appropriate, and that the most useful time to run the ORC engine may be during the earlier, mid-afternoon hours of 15:00 to 17:00 (and possibly again in the later evening after 21:00). In winter when the daily solar-energy gain on the average day is smaller and the domestic electricity load profile is closer in shape to that for the UK, a full-storage strategy can be employed to offset the entire ORC run time to evening hours.

3.5. Comparison of PCM and sensible TES media

In order to provide a preliminary performance assessment of potential TES material options for use with the S-CHP system, a simple system model is devised based on a 15 m^2 array of EFPC modules, an ORC engine sized for a nominal electrical output of 1 kW, and a zero-dimensional (lumped) TES vessel of a specified total volume. The system is simulated for a clear summer day in July, selected from the London UK climate dataset and presented in Fig. 10. The simulation is performed at time-step interval of 1 min.

The range of sensible and latent TES materials and their properties are listed in Table 2. The physical properties chosen for the PCMs are broadly representative of a range of organic and inorganic (hydrated-salt based) materials [39]. The PCM melting temperature is chosen as the optimal summertime collector inlet-temperature from Fig. 6a. For the sensible storage options using solid media (granite and quartzite), it is assumed that the TES takes the form of a packed bed of crushed particles with a low porosity of 22% [9], and that the void space is occupied by the heat-transfer fluid that flows through the store transferring thermal energy from

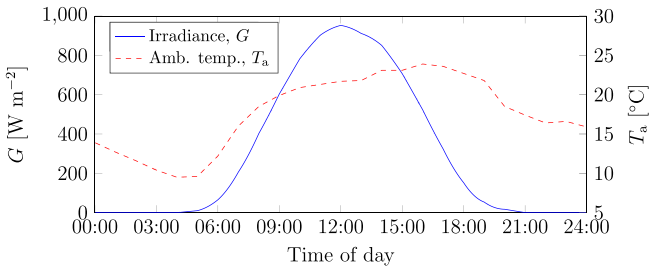


Fig. 10. Irradiance and ambient temperature profiles used for the diurnal simulation (UK peak solar day in July: mean irradiance on 36°, tilted plane = 309 W m^{-2}, mean temperature = 17.8 °C, maximum irradiance on 36°, tilted plane = 952 W m^{-2}, maximum temperature = 23.9 °C).

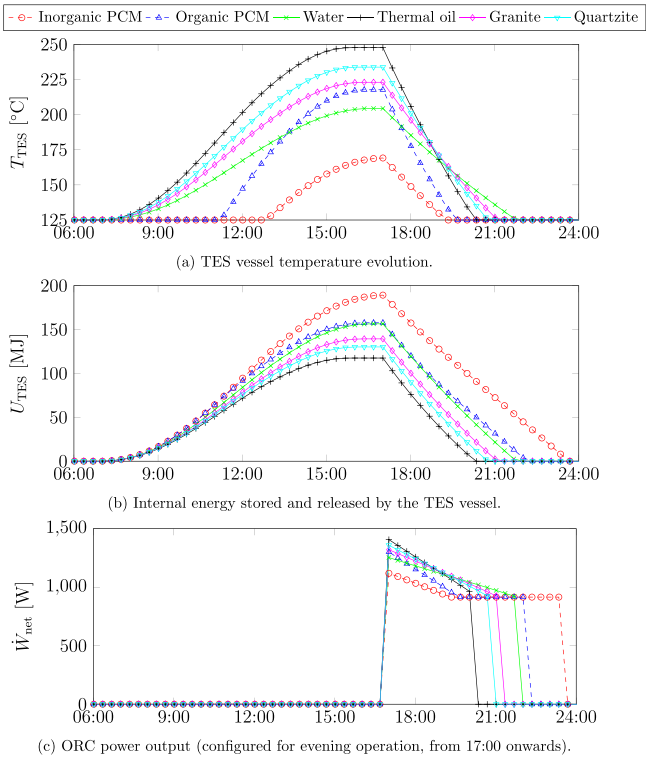
Table 2
Thermal energy storage (TES) material physical properties.

	ρ, kg m^{-3}	Δh_{pc}, kJ kg^{-1}	c, kJ kg^{-1} K^{-1}
Inorganic PCM[a]	1560	154	2.00
Organic PCM[a]	825	171	2.27
Water (liquid)[b]	940	–	4.25
Thermal oil[b]	940	–	1.92
Quartzite	2500	–	0.83
Granite	2640	–	1.02

[a] Property values listed for PCMs are representative the range of existing commercially available organic aliphatic compounds and inorganic hydrated-salt products in Ref. [39].
[b] Property values listed correspond to a fluid temperature of 125 °C, and (in the case of water) a fluid pressure of 20 bar.

the collector array to the storage media. The system operation is based on the full-storage strategy in which the operation of the ORC engine is offset to the evening hours (17:00 is chosen as the start of the engine's operating period). The purpose of the simulation is to compare, for each TES option, the total-work output provided by the ORC engine over a daily simulation period. As a simplification, thermal losses are neglected and the initial condition of the store is set as the minimum temperature required to run the ORC engine. In the case of the PCMs, the initial condition is assumed to be fully solidified/frozen and the internal energy increases isothermally at first as melting of the PCM occurs. When the PCM is fully melted, the TES stores heat sensibly and its temperature increases. As the temperature of the store increases, the inlet temperature to the collector also increases and the collector efficiency decreases. Meanwhile the heat-source temperature to the ORC engine also increases, causing the ORC power-output to increase.

In Fig. 11, results are shown for a 500-L TES volume. The inorganic (salt-based) PCM experiences the lowest maximum



(a) TES vessel temperature evolution.

(b) Internal energy stored and released by the TES vessel.

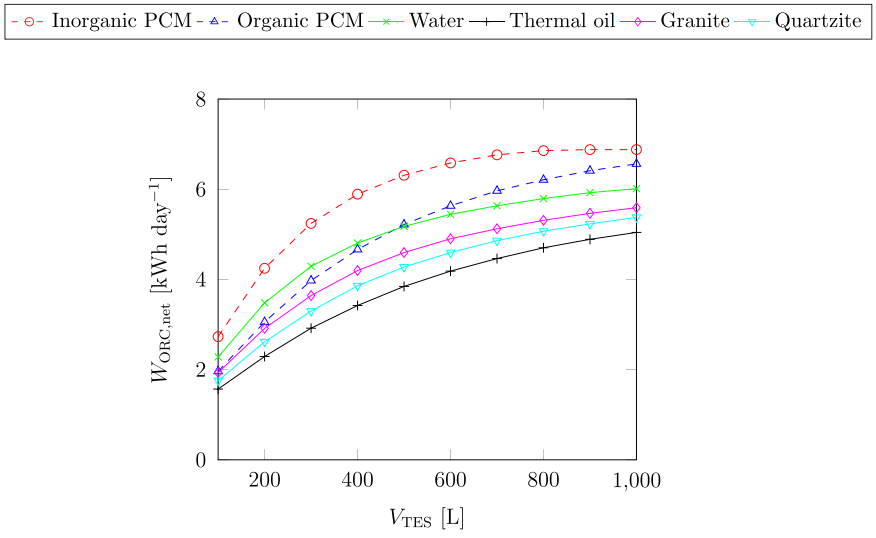
(c) ORC power output (configured for evening operation, from 17:00 onwards).

Fig. 11. Diurnal performance simulation results for the S-CHP system with various TES options on a clear-sky summer day, with a 15-m^2 EFPC solar-array and a 500-L nominal TES volume. The system is operated in full-storage mode, with a 1-kW ORC engine whose operation period is shifted to evening hours, starting at 17:00.

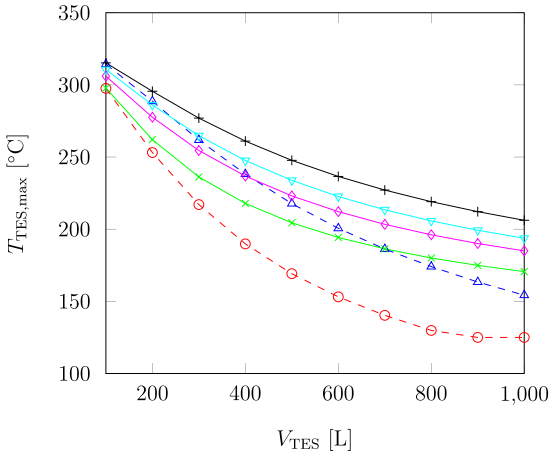
storage-temperature (169 °C) and, hence, the lowest inlet-temperatures to the collector array, the highest collector efficiencies and highest solar-energy gains (since collector losses increase at higher operating temperatures). The inorganic PCM experiences a lower maximum temperature than the organic PCM because of its higher (volumetric) latent-heat, which means that it is able store heat isothermally over a longer period. Due to its high specific heat-capacity, water is found to reach a lower maximum temperature than the other sensible storage-media and the organic PCM, but not the inorganic PCM; however, the storage temperature is still high enough that significant pressurisation (16 bar at 200 °C) would be required to maintain the water in the liquid phase. Thermal oil has the lowest specific heat-capacity and, as such, experiences the largest temperature swing over the daily period, the highest maximum storage-temperature, the highest inlet-temperatures to the collector array and the lowest collector-efficiencies.

Further, higher TES temperatures result in higher initial power-outputs at the start of the ORC-engine operation period (Fig. 11c), due to the increased superheating at the expander inlet. However, the total-work output and the duration of the operating period are higher for the materials with the lower storage temperatures. The inorganic PCM is associated with a 25% higher total-work output than the best sensible storage-medium, and delivers an average net-power of 0.95 kW over a continuous operation-period of 6 h and 38 min.

Fig. 12 shows the daily variation in the work output from the ORC engine over a range of TES volumes from 100 L to 1000 L. For the inorganic PCM, an 850-L TES vessel or larger provides sufficient volume to store the full quantity of solar energy collected over the daily period isothermally (this is approximately in agreement with the TES vessel size requirement for full storage with inorganic PCMs in Fig. 8b). For storage volumes below 850 L, some of the solar energy is stored sensibly, causing the maximum temperature of the store to rise above the melting temperature of the material. At the smallest value of the TES volume (100 L), 69% of the thermal energy input to the PCM-TES vessel is taken up as sensible heat, with the result that there is little difference between the maximum storage-temperature for the PCMs and the sensible storage media. However, the daily net-work output



(a) Daily ORC work output as a function of TES volume.



(b) Daily maximum storage temperature as a function of TES volume

Fig. 12. ORC daily work output and maximum storage temperature as functions of TES volume, for a clear-sky (UK) summer day and the S-CHP system configured with a 15-m^2 EFPC solar-array.

Table 3
Summary of S-CHP system capital costs.

Item	Cost	Equation
TES costs		
Hydrated-salt PCM (400 L) [34]	£1560	$2.5 \cdot m_{pcm}$
Insulated tank [34]	£780	0.5· PCM cost
ORC main system component costs		
Expander[a]	£1750	$78 + 298 \cdot 10^{-3} \cdot \dot{V}_{sw,exp}$
Pump[b]	£320	$275 + 0.55 \cdot \dot{W}_{pp,orc}$
Heat exchangers[c]	£350	$158 + 258 \cdot A_{hx}$
Air-cooled heat exchanger [40]	£420	$75 \cdot \dot{Q}_{cond}$
Working fluid [41]	£240	$25 \cdot m_{fluid}$
Liquid receiver tank (5 L) [42]	£90	
Generator [43]	£450	
Area-related solar-thermal system costs		
Evacuated tube collector array (ETHPC)	£1875	$125 \cdot A_{sc}$
Evacuated flat-plate collector (EFPC)	£2500	$170 \cdot A_{sc}$
Circulation pump [44]	£95	$70 + 0.53 \cdot \dot{W}_{pp,sc}$
Supporting framework [45]	£150	$10 \cdot A_{sc}$
Pipework and valves [45]	£75	$5 \cdot A_{sc}$
Heat transfer fluid [45]	£95	$6.25 \cdot A_{sc}$
Non-area-related ancillary costs		
Hot water tank[d] [40]	£690	$4600 \cdot V_{tank}$
Expansion vessel (25 L) [46]	£50	50
Instrumentation and controls [45]	£250	250
Installation cost	£1500	0.2 · PEC

[a] Based on costs for small-scale positive-displacement compressors (piston, screw, scroll) related to swept volume.
[b] Based on costs for equivalent-sized vane pumps and diaphragm pumps, related to hydraulic power.
[c] Based on costs for small brazed-plate heat exchangers, related to heat exchanger surface area.
[d] Based on a Grade 2 specification 150 L domestic cylinder, tested to 2.2 bar, 15 m maximum head.

from the ORC engine is still 20% higher for the inorganic PCM compared to the best sensible-storage medium, which is pressurised liquid water, and 41% higher than the best solid TES medium, which is granite.

3.6. System costs

Table 3 shows a cost breakdown of the system components based on the results of a market analysis and literature review. The data from the market analysis were used to form cost correlations based on a dominant sizing variable that was identified from the data. For example, in the case of the solar-collector array the cost is related to the array area, while for the ORC expander, the cost is related to the volumetric flow-rate at the expander exhaust which determines the overall size of the machine. For the TES, costs are based on the equivalent raw material costs for inorganic (salt-based) PCMs and the cost of an insulated storage tank. The volume chosen for the TES in the analysis is 400 L, based on the requirement for summertime full storage in London found in the analysis in Section 3.3. The cost of the tank is estimated to be approximately 50% of the raw PCM cost [47]. The system installation cost is assumed to be 20% of the total purchased equipment cost (PEC) [48].

It is found that the addition of the PCM thermal energy storage vessel leads to a ~30% increase in the total installed cost of the system. The estimated cost of the TES (PCM + tank) is £2340, compared to £3650 for the solar array sub-system (including the 15 m^2 EFPC array, domestic hot water cylinder and ancillaries), and £3600 for the ORC sub-system (nominal 1 kW_e output, including working fluid and AC generator). The reduction in price as a result of choosing the ETHPC instead of the EFPC array is difficult to assess due to the wide range of collector prices found in the literature and from various suppliers. A conservative cost of 125 £/m^2 is chosen here for the ETHPC which is broadly representative evacuated tube prices found in Europe; however in China evacuated tubes prices can be as low as 25 £/m^2 due to the lower cost of manufacturing [49–52]. Meanwhile the higher cost for the EFPC is based on the projected cost of the technology upon reaching market maturity, comparable with that of standard glazed (non-evacuated) FPC [53]. The ORC system components, in particular the expander, represent a significant potential for cost reductions in the future. Many of the kiloWatt-scale expanders currently being developed for ORCs are based on reversed scroll designs; however reciprocating-piston expanders have the potential to be developed as cheaper alternatives. Furthermore, the cost of the entire system can potentially be reduced due to the economy of scale associated with mass-production. The costs obtained from the market analysis are mostly obtained as single-unit prices. With the likelihood that system suppliers will purchase the components in bulk quantities, it can be predicted with reasonable certainty that the cost to produce the system will be lower than the estimate provided from this analysis. This extends in particular to the TES, with the PCM cost estimated to reduce by an order of magnitude when purchased by the tonne rather than by the kilogram [54].

Low-cost filler materials such as rock particles (builder's aggregate) are available in bulk quantities at costs in the range 30–50 £/tonne (0.03–0.05 £/kg) [55]. On a mass basis, this is around 2% of the cost of the hydrated-salt PCMs cited above. Although this is a highly significant reduction in the cost of the storage medium, once the cost of the containment vessel is also accounted for, the cost of TES now represents an addition of ~10% to the overall cost of a S-CHP system, compared to ~30% for the PCM-TES case.

4. Conclusions and further work

The analysis presented in this paper has been concerned with evaluating a range of sensible- and latent-TES options for use in a solar, combined heat and power system based on an ORC engine. The S-CHP system evaluated here was considered for operation in the contrasting climates of Cyprus and the UK, and was constrained to a solar-collector array size equivalent to a domestic rooftop area of 15 m^2. An effort has been made to address questions surrounding the overall operation and performance of the S-CHP system, in particular focussing on its electricity-generating performance, as well as the selection and design of different non-concentrating solar-thermal collector types and TES solutions.

Overall S-CHP system solar-to-electrical conversion efficiencies in the range 4.4–6.4% have been predicted in the UK and 6.3–7.3% in Cyprus (higher in warmer months) when employing evacuated flat-plate collectors. On the other hand, a system based on low-cost evacuated-tube heat-pipe collectors has been shown to deliver approximately half of the aforementioned efficiencies in both the UK and Cyprus climates. Furthermore, the used of evacuated flat-plate collectors in a S-CHP system in the UK has the potential to provide 4 h of continuous operation at an electrical power output of 1-kW over an average day in July, 3 h in April and 0.75 h in January. In the Cyprus climate, the S-CHP system has the potential to provide 7 h of continuous 1-kW power output over an average day in July, 6 h in April and 3 h January.

PCMs for latent thermal energy storage have been shown to provide a superior power-output from the S-CHP system for a smaller equivalent storage volume than water (our benchmark sensible-energy storage medium), and also low-cost packed-bed using granite and quartzite rock particles. However, the performance advantage that can be achieved with PCMs is dependent on the selection of a suitable product with a melting temperature that is matched to the optimal operating-temperatures of the

collector and ORC engine. Hydrated-salt PCMs show advantages over organic PCMs both in terms of cost and volumetric heat-capacity during phase change.

By designing the system for "partial storage" in order to provide buffered, continuous operation during daylight hours, the resulting summertime nominal net-power output in both Cyprus and the UK is below 1 kW, which is typically the lower limit of "small-scale" systems described in the ORC literature. On the other hand, designing the system for "full storage" in order to prioritise evening operation of the ORC engine, results in larger storage volumes that may be impractical for domestic applications in terms of cost and space availability. The work has highlighted the requirement for a bespoke small-scale expander to match the large volume ratios (>10) required for optimal S-CHP system operation in the summertime design condition (commercially available and experimental small-scale positive-displacement expanders based on scroll machines tend to have built-in volume ratios <5).

In the UK climate, the full-storage solution with an inorganic hydrated-salt PCM-TES requires a storage volume of ~400 L when sized for an average summer day. In Cyprus, the volume required for full storage on an average summer day is more than double that for the UK, and as a result a partial-storage (buffer-storage) strategy may be preferred, whereby the ORC engine and solar array are operated simultaneously. This may also present further advantages in Cyprus, where daytime domestic electricity demand is significant due to air-conditioning in summer, compared to the UK where the evening peak in domestic demand is prevalent throughout the year.

A TES volume of 400 L with hydrated-salt PCM as the storage medium represents a TES cost of ~£2300 (based on 1.5–3.5 £/kg for the PCM) and could lead to an increased capital cost of ~30% compared to a system without TES. This is a significantly lower cost than the equivalent electricity-storage solution (e.g., with batteries[1]), which highlights one of the key advantages of S-CHP systems over PV equivalents, in addition to the ability to deliver a thermal output for hot-water and/or space heating. Sensible storage using water eliminates the high cost of the PCM storage media, although the cost of the containment is likely to be considerably higher due to the pressurisation required. Sensible storage using a solid packed-bed (with bulk quantity prices for hardcore/aggregate in the range 0.03–0.05 £/kg) could present the lowest capital-cost feasible option, at the expense of a larger temperature swing over the diurnal period and the associated reduction in solar-to-electrical energy conversion, which here was estimated to be 20–30% compared to the hydrated-salt PCM for the full-storage strategy in summer conditions.

A full evaluation and comparison of the various sensible- and latent-heat storage strategies requires a detailed thermal model in which the various operational strategies can be fully explored. In this study, a lumped model of the TES tank was used to provide a simplified comparison of the various media. The lumped approach is likely to have resulted in an overestimate of the temperatures in the collector array for the sensible storage media, which in a typical stratified storage configuration is fed with fluid from the cooler bottom zone of the tank. A detailed analysis should be undertaken in future work to examine the performance of a stratified TES tank using a one-dimensional discretised model, as well as the optimisation of the tank dimensions and the S-CHP system operational strategy to maximise the solar-to-electrical efficiency over the diurnal storage cycle, and to compare this with alternative competing solutions, e.g., based on PV and hybrid PV-thermal panels [48,59]. For the PCM, it is also important to consider the heat exchanger design, and models of embedded heat exchangers versus packed-bed heat exchangers using encapsulated PCM should also be compared in future work.

[1] Tesla's (one-size) 14-kW h Powerwall 2 is estimated at more than £6000 [56], while the 6-kW h Powervault Li-ion battery costs around £5000 to install (including taxes) [57,58].

Acknowledgement

This work was supported by the UK Engineering and Physical Sciences Research Council (EPSRC) [Grant Nos. EP/K502856/1 and EP/P004709/1]. Data supporting this publication can be obtained on request from cep-lab@imperial.ac.uk.

References

[1] C.N. Markides, The role of pumped and waste heat technologies in a high-efficiency sustainable energy future for the UK, Appl. Thermal Eng. 53 (2) (2013) 197–209.
[2] A. Ramos, I. Guarracino, A. Mellor, D. Alonso-Álvarez, P.R.N. Childs, N.J. Ekins-Daukes, C.N. Markides, Solar-Thermal and Hybrid Photovoltaic-Thermal Systems for Renewable Heating , Grantham Institute Briefing Paper, May 2017, Available from: https://www.imperial.ac.uk/grantham/publications/ (accessed 10 Aug. 2017).
[3] J. Freeman, K. Hellgardt, C.N. Markides, An assessment of solar-thermal collector designs for small-scale combined heating and power applications in the United Kingdom, Heat Transf. Eng. 36 (14–15) (2015) 1332–1347.
[4] C.N. Markides, Low-concentration solar-power systems based on organic Rankine cycles for distributed-scale applications: Overview and further developments, Front. Energy Res. 3 (2015) 47.
[5] J. Freeman, K. Hellgardt, C.N. Markides, An assessment of solar-powered organic Rankine cycle systems for combined heating and power in UK domestic applications, Appl. Energy 138 (2015) 605–620.
[6] J. Freeman, K. Hellgardt, C.N. Markides, Working fluid selection and electrical performance optimisation of a domestic solar-ORC combined heat and power system for year-round operation in the UK, Appl. Energy 186 (2017) 291–303.
[7] B. Kelly, D. Kearney, Thermal Storage Commercial Plant Design Study for a 2-tank Indirect Molten Salt System, Tech. Rep., NREL/SR-550-40166, July 2006.
[8] G. Heath, C. Turchi, T. Decker, J. Burkhardt, C. Kutscher, Life cycle assessment of thermal energy storage: Two-tank indirect and thermocline, in: ASME 2009 3rd International Conference on Energy Sustainability collocated with the Heat Transfer and InterPACK09 Conferences, American Society of Mechanical Engineers, 2009, pp. 689–690.
[9] J.-F. Hoffmann, T. Fasquelle, V. Goetz, X. Py, A thermocline thermal energy storage system with filler materials for concentrated solar power plants: Experimental data and numerical model sensitivity to different experimental tank scales, Appl. Therm. Eng. 100 (2016) 753–761.
[10] R. Chacartegui, L. Vigna, J. Becerra, V. Verda, Analysis of two heat storage integrations for an organic Rankine cycle parabolic trough solar power plant, Energy Convers. Manage. 125 (2016) 353–367.
[11] S. Canada, G. Cohen, R. Cable, D. Brosseau, H. Price, Parabolic trough organic Rankine cycle solar power plant, in: DOE Solar Energy Technologies Program Review Meeting, Denver, USA, 2004.
[12] G.J. Kolb, V. Hassani, Performance analysis of thermocline energy storage proposed for the 1 MW Saguaro solar trough plant, in: ASME 2006 International Solar Energy Conference, American Society of Mechanical Engineers, 2006, pp. 1–5.
[13] S. Quoilin, M. Orosz, H. Hemond, V. Lemort, Performance and design optimization of a low-cost solar organic Rankine cycle for remote power generation, Sol. Energy 85 (5) (2011) 955–966.
[14] E. Casati, A. Galli, P. Colonna, Thermal energy storage for solar-powered organic Rankine cycle engines, Sol. Energy 96 (2013) 205–219.
[15] T. Pirasaci, D.Y. Goswami, Influence of design on performance of a latent heat storage system for a direct steam generation power plant, Appl. Energy 162 (2016) 644–652.
[16] A. Gupta, R. Mathie, C.N. Markides, An experimental and computational investigation of a thermal storage system based on a phase change material: Heat transfer and performance characterization, Comput. Therm. Sci.: Int. J. 6 (4) (2014).
[17] G. Manfrida, R. Secchi, K. Stańczyk, Modelling and simulation of phase change material latent heat storages applied to a solar-powered organic Rankine cycle, Appl. Energy 179 (2016) 378–388.
[18] M. Naghavi, K. Ong, I. Badruddin, M. Mehrali, M. Silakhori, H. Metselaar, Theoretical model of an evacuated tube heat pipe solar collector integrated with phase change material, Energy 91 (2015) 911–924.
[19] W.D. Steinmann, M. Eck, Buffer storage for direct steam generation, Sol. Energy 80 (10) (2006) 1277–1282.
[20] L. Jing, P. Gang, J. Jie, Optimization of low temperature solar thermal electric generation with organic Rankine cycle in different areas, Appl. Energy 87 (11) (2010) 3355–3365.
[21] UK Energy Research Centre, Electricity User Load Profiles by Profile Class, November 1997. Available from: <http://data.ukedc.rl.ac.uk/simplebrowse/edc/efficiency/residential/LoadProfile> (accessed 1 Feb. 2017).
[22] Promotion of PV Energy Through Net Metering Optimization: Existing Initiatives, Tariffs and PV Potential in Cyprus, Spain, Greece, Slovenia,

Portugal and France. WP3 No [D 3.1], Tech. Rep., PV-NET Project Report. Project Reference Number 5023, May 2014.
[23] Office of Gas and Electricity Markets, Typical Domestic Energy Consumption Values, 2015, Available: <https://www.ofgem.gov.uk> (accessed 15 Feb. 2017).
[24] P. Owen, Powering the Nation. Household Electricity-using Habits Revealed, Energy Saving Trust/DECC/DEFRA, London, 2012.
[25] Y. Wang, F. Ronilaya, X. Chen, A.P. Roskilly, Modelling and simulation of a distributed power generation system with energy storage to meet dynamic household electricity demand, Appl. Therm. Eng. 50 (1) (2013) 523–535.
[26] D. Serghides, S. Dimitriou, M. Katafygiotou, Towards European targets by monitoring the energy profile of the Cyprus housing stock, Energy Build. 132 (2016) 130–140.
[27] TVP Solar, HT-Power Product Datasheet, 2013, Available from: <http://www.tvpsolar.com> (accessed 24 Feb. 2015).
[28] Kinspan Thermomax, HP200 Heat Pipe Vacuum Tube Solar Collector Product Datasheet, 2017, Available from: <http://www.kingspansolar.ie/pdf/HP200.pdf> (accessed 15 Feb. 2017).
[29] Energy Saving Trust, Solar Energy Calculator Sizing Guide, February 2015, Available from: <http://www.pvfitcalculator.energysavingtrust.org.uk/Documents/150224_SolarEnergy_Calculator_Sizing_Guide_v1.pdf>.
[30] ASHRAE, International Weather for Energy Calculations (IWEC) Weather Files, Users Manual and CD-ROM, 2001.
[31] J.E. Nielsen, R. Berkmann, The Solar Keymark, in: Proceedings of EUROSUN 2000, Copenhagen, Denmark, 2000.
[32] BS EN 12975-2: 2006, Thermal Solar Systems and Components. Solar Collectors. Test Methods.
[33] X. Wang, L. Zhao, J. Wang, W. Zhang, X. Zhao, W. Wu, Performance evaluation of a low-temperature solar Rankine cycle system utilizing R245fa, Sol. Energy 84 (3) (2010) 353–364.
[34] Z. Ure, Personal Communication, Phase Change Material Products, Ltd., January 2017.
[35] R. Kempener, J. Burch, C. Navntoft, D. Mugnier, J.E. Nielsen, W. Weiss, Solar Heating and Cooling for Residential Applications, Tech. Rep., IEA-ETSAP and IRENA Technology Brief, January 2015.
[36] S.A. Kalogirou, Solar water heaters in Cyprus: Manufacturing, performance and applications, in: Proceedings of the 4th Congress on Energy Conservation in Buildings and Renewable Energy, Tehran, Iran, 2005.
[37] J. Bao, L. Zhao, A review of working fluid and expander selections for organic Rankine cycle, Renew. Sustain. Energy Rev. 24 (2013) 325–342.
[38] Air Squared, E15H022A-SH 1 kW Semi-hermetic Scroll Expander. Product Datasheet and Connection Drawings, Available from: <http://www.airsquared.com> (accessed 11 Nov. 2016).
[39] Phase Change Material Products, Ltd., United Kingdom Products Catalogue, 2013, Available from: <http://www.pcmproducts.net> (accessed 27 Nov. 2016).
[40] Davis Langdon LLP (Ed.), Spon's Mechanical and Electrical Services Price, 41st ed., CRC Press, London, United Kingdom and New York, NY, USA, 2010.
[41] P. Dinnage, Personal Communication, Climalife IDS Refrigeration, Ltd., July 2016.
[42] S. Quoilin, Sustainable Energy Conversion Through the Use of Organic Rankine Cycles for Waste Heat Recovery and Solar Applications (Ph.D. thesis), University of Liège, Belgium, 2011.
[43] Government Industrial Supply, List Price for Voltmaster AB30 Belt-driven Generator, Available from: <http://store.gissn.com> (accessed 14 Sept. 2016).
[44] Plumb Center, UK, List Prices for Grundfos UPS2 Circulator Pumps, Available from: <http://www.plumbcenter.co.uk> (accessed 6 Sept. 2016).
[45] Origen Energy Ltd., List Price for Kingspan Thermomax Solar Evacuated Tube Hot Water Systems and Components, Available from: <http://www.origen.ie> (accessed 6 Sept. 2016).
[46] Screwfix, List Prices for Plumbing Supplies and Hot Water System Components, Available from: <http://www.screwfix.com> (accessed 6 Sept. 2016).
[47] J.N. Chiu, Heat Transfer Aspects of Using Phase Change Material in Thermal Energy Storage Applications (Master's Thesis), KTH Royal Institute of Technology, 2011.
[48] M. Herrando, C.N. Markides, Hybrid PV and solar-thermal systems for domestic heat and power provision in the UK: Techno-economic considerations, Appl. Energy 161 (2016) 512–532.
[49] J. Han, A.P. Mol, Y. Lu, Solar water heaters in China: A new day dawning, Energy Policy 38 (1) (2010) 383–391.
[50] S. Qiu, M. Ruth, S. Ghosh, Evacuated tube collectors: A notable driver behind the solar water heater industry in China, Renew. Sustain. Energy Rev. 47 (2015) 580–588.
[51] X. Liu, W. Chen, M. Gu, S. Shen, G. Cao, Thermal and economic analyses of solar desalination system with evacuated tube collectors, Sol. Energy 93 (2013) 144–150.
[52] L. Ayompe, A. Duffy, M. Mc Keever, M. Conlon, S. McCormack, Comparative field performance study of flat plate and heat pipe evacuated tube collectors (ETCs) for domestic water heating systems in a temperate climate, Energy 36 (5) (2011) 3370–3378.
[53] J. Isles, A leap forward for solar thermal panels, Energy Indust. Times 5 (1) (2012) 15.
[54] A. Hasan, S.J. McCormack, M.J. Huang, B. Norton, Energy and cost saving of a photovoltaic-phase change materials (PV-PCM) system through temperature regulation and performance enhancement of photovoltaics, Energies 7 (3) (2014) 1318–1331.
[55] Building Supplies Online, Loose Load Aggregate by the Tonne, Available from: <http://www.building-supplies-online.co.uk/building-materials> (accessed 14 Feb. 2017).
[56] Tesla, Powerwall 2, 2017, Available from: <https://www.tesla.com> (accessed 1 Mar. 2017).
[57] Powervault, G200 Li-ion 6 kW h, Technical Specification, 2017, Available from: <http://www.powervault.co.uk> (accessed 1 Mar. 2017).
[58] Powervault, G200 Trade Price List, March 2017, [Personal communication].
[59] M. Herrando, C.N. Markides, K. Hellgardt, A UK-based assessment of hybrid PV and solar-thermal systems for domestic heating and power: System performance, Appl. Energy 122 (2014) 288–309.